In conclusion, our study found that the reduction of Tregs in tumors contributes to induction of antitumor immunity by type I IFN. Intratumoral IFN-α gene transfer is a promising immunotherapy for solid cancers, because of the activation of tumor-specific immunity, suppression of the immunotolerant environment and excellent safety features. This therapeutic strategy is deserving of an evaluation in future clinical trials for solid cancers.

CONFLICT OF INTEREST

The authors declare no conflict of interest.

REFERENCES

1 Gonzalez-Navajas JM, Lee J, David M, Raz E. Immunomodulatory functions of type I interferons. Nat Rev Immunol 2012; 12: 125–135.
2 Ferrantini M, Capone I, Belardelli F. Interferon-alpha and cancer: mechanisms of action and new perspectives of clinical use. Biochimie 2007; 89: 884–893.
3 Rizza P, Moretti F, Belardelli F. Recent advances on the immunomodulatory effects of IFN-alpha: implications for cancer immunotherapy and autoimmunity. Autoimmunity 2010; 43: 204–209.
4 Escobar G, Moi D, Ranghetti A, Ozkal-Baydin P, Squadrito ML, Kajaste-Rudnitski A et al. Genetic engineering of hematopoiesis for targeted IFN-alpha delivery inhibits breast cancer progression. Sci Transl Med 2014; 6: 217ra3.
5 Narumi K, Kondoh A, Udagawa T, Hara H, Goto N, Ikarashi Y et al. Administration route-dependent induction of antitumor immunity by interferon-alpha gene transfer. Cancer Sci 2010; 101: 1686–1694.
6 Ohashi M, Yoshida K, Kushida M, Miura Y, Ohnami S, Ikarashi Y et al. Adenovirus-mediated interferon alpha gene transfer induces regional direct cytotoxicity and possible systemic immunity against pancreatic cancer. Bri J Cancer 2005; 93: 441–449.
7 Hatanaka K, Suzuki K, Miura Y, Yoshida K, Ohnami S, Kitade Y et al. Interferon-alpha and antisense K-ras RNA combination gene therapy against pancreatic cancer. J Gene Med 2004; 6: 1139–1148.
8 Hara H, Kobayashi A, Yoshida K, Ohashi M, Ohnami S, Uchida E et al. Local interferon-alpha gene therapy elicits systemic immunity in a syngeneic pancreatic cancer model in hamster. Cancer Sci 2007; 98: 455–463.
9 Udagawa T, Narumi K, Goto N, Aida K, Suzuki K, Ochiya T et al. Syngeneic hematopoietic stem cell transplantation enhances the antitumor immunity of intratumoral type I interferon gene transfer for sarcoma. Hum Gene Ther 2012; 23: 173–186.
10 Belardelli F, Ferrantini M, Proietti E, Kirkwood JM. Interferon-alpha in tumor immunity and immunotherapy. Cytokine Growth Factor Rev 2002; 13: 119–134.
11 Burdick LM, Somani N, Somani AK. Type I IFNs and their role in the development of autoimmune diseases. Expert Opin Drug Saf 2009; 8: 459–472.
12 Santini SM, Lapenta C, Santodonato L, D'Agostino G, Belardelli F, Ferrantini M. IFN-alpha in the generation of dendritic cells for cancer immunotherapy. Handb Exp Pharmacol 2009; 188: 295–317.
13 Kobayashi N, Hiraoka N, Yamagami W, Ojima H, Kanai Y, Kosuge T et al. FOXP3+ regulatory T cells affect the development and progression of hepatocarcinogenesis. Clin Cancer Res 2007; 13: 902–911.
14 Jacobs JF, Nierkens S, Figdor CG, de Vries IJ, Adema GJ. Regulatory T cells in melanoma: the final hurdle towards effective immunotherapy? Lancet Oncol 2012; 13: e32–e42.
15 Byrne WL, Mills KH, Lederer JA, O'Sullivan GC. Targeting regulatory T cells in cancer. Cancer Res 2011; 71: 6915–6920.
16 Lal G, Zhang N, van der Touw W, Ding Y, Ju W, Bottinger EP et al. Epigenetic regulation of Foxp3 expression in regulatory T cells by DNA methylation. J Immunol 2009; 182: 259–273.
17 Cucak H, Yrlid U, Reizis B, Kalinke U, Johansson-Lindbom B. Type I interferon signaling in dendritic cells stimulates the development of lymph-node-resident T follicular helper cells. Immunity 2009; 31: 491–501.

18 Sato E, Olson SH, Ahn J, Bundy B, Nishikawa H, Qian F et al. Intraepithelial CD8+ tumor-infiltrating lymphocytes and a high CD8+/regulatory T cell ratio are associated with favorable prognosis in ovarian cancer. Proc Natl Acad Sci USA 2005; 102: 18538–18543.
19 Gnerlich JL, Mitchem JB, Weir JS, Sankpal NV, Kashiwagi H, Belt BA et al. Induction of Th17 cells in the tumor microenvironment improves survival in a murine model of pancreatic cancer. J Immunol 2010; 185: 4063–4071.
20 Sharma MD, Hou DY, Liu Y, Koni PA, Metz R, Chandler P et al. Indoleamine 2,3-dioxygenase controls conversion of Foxp3+ Tregs to TH17-like cells in tumor-draining lymph nodes. Blood 2009; 113: 6102–6111.
21 Bacher N, Raker V, Hofmann C, Graulich E, Schwenk M, Baumgrass R et al. Interferon-alpha suppresses cAMP to disarm human regulatory T cells. Cancer Res 2013; 73: 5647–5656.
22 Bacher N, Graulich E, Jonuleit H, Grabbe S, Steinbrink K. Interferon-alpha abrogates tolerance induction by human tolerogenic dendritic cells. PloS One 2011; 6: e22763.
23 Pace L, Vitale S, Dettori B, Palombi C, La Sorsa V, Belardelli F et al. APC activation by IFN-alpha decreases regulatory T cell and enhances Th cell functions. J Immunol 2010; 184: 5969–5979.
24 Dong C. TH17 cells in development: an updated view of their molecular identity and genetic programming. Nat Rev Immunol 2008; 8: 337–348.
25 Ivanov II, McKenzie BS, Zhou L, Tadokoro CE, Lepelley A, Lafaille JJ et al. The orphan nuclear receptor RORgammat directs the differentiation program of proinflammatory IL-17+ T helper cells. Cell 2006; 126: 1121–1133.
26 Yang XO, Pappu BP, Nurieva R, Akimzhanov A, Kang HS, Chung Y et al. T helper 17 lineage differentiation is programmed by orphan nuclear receptors ROR alpha and ROR gamma. Immunity 2008; 28: 29–39.
27 Xu L, Kitani A, Fuss I, Strober W. Cutting edge: regulatory T cells induce CD4+CD25-Foxp3- T cells or are self-induced to become Th17 cells in the absence of exogenous TGF-beta. J Immunol 2007; 178: 6725–6729.
28 Yang XO, Nurieva R, Martinez GJ, Kang HS, Chung Y, Pappu BP et al. Molecular antagonism and plasticity of regulatory and inflammatory T cell programs. Immunity 2008; 29: 44–56.
29 Zheng SG, Wang J, Horwitz DA. Cutting edge: Foxp3+CD4+CD25+ regulatory T cells induced by IL-2 and TGF-beta are resistant to Th17 conversion by IL-6. J Immunol 2008; 180: 7112–7116.
30 Bollrath J, Phesse TJ, von Burstin VA, Putoczki T, Bennecke M, Bateman T et al. gp130-mediated Stat3 activation in enterocytes regulates cell survival and cell-cycle progression during colitis-associated tumorigenesis. Cancer Cell 2009; 15: 91–102.
31 Grivennikov S, Karin M. Autocrine IL-6 signaling: a key event in tumorigenesis? Cancer Cell 2008; 13: 7–9.
32 Grivennikov S, Karin E, Terzic J, Mucida D, Yu GY, Vallabhapurapu S et al. IL-6 and Stat3 are required for survival of intestinal epithelial cells and development of colitis-associated cancer. Cancer Cell 2009; 15: 103–113.
33 Naugler WE, Karin M. The wolf in sheep's clothing: the role of interleukin-6 in immunity, inflammation and cancer. Trends Mol Med 2008; 14: 109–119.
34 Bromberg J, Wang TC. Inflammation and cancer: IL-6 and STAT3 complete the link. Cancer Cell 2009; 15: 79–80.
35 Anglesio MS, George J, Kulbe H, Friedlander M, Rischin D, Lemech C et al. IL6-STAT3-HIF signaling and therapeutic response to the angiogenesis inhibitor sunitinib in ovarian clear cell cancer. Clin Cancer Res 2011; 17: 2538–2548.
36 Kulbe H, Thompson R, Wilson JL, Robinson S, Hagemann T, Fatah R et al. The inflammatory cytokine tumor necrosis factor-alpha generates an autocrine tumor-promoting network in epithelial ovarian cancer cells. Cancer Res 2007; 67: 585–592.
37 Song L, Rawal B, Nemeth JA, Haura EB. JAK1 activates STAT3 activity in non-small-cell lung cancer cells and IL-6 neutralizing antibodies can suppress JAK1-STAT3 signaling. Mol Cancer Ther 2011; 10: 481–494.
38 Guo Y, Nemeth J, O'Brien C, Susa M, Liu X, Zhang Z et al. Effects of siltuximab on the IL-6-induced signaling pathway in ovarian cancer. Clin Cancer Res 2010; 16: 5759–5769.
39 Chari A, Pri-Chen H, Jagannath S. Complete remission achieved with single agent CNTO 328, an anti-IL-6 monoclonal antibody, in relapsed and refractory myeloma. Clin Lymphoma Myeloma Leukemia 2013; 13: 333–337.
40 Rossi JF, Negrier S, James ND, Kocak I, Hawkins R, Davis H et al. A phase I/II study of siltuximab (CNTO 328), an anti-interleukin-6 monoclonal antibody, in metastatic renal cell cancer. Bri J Cancer 2010; 103: 1154–1162.
41 Fizazi K, De Bono JS, Flechon A, Heidenreich A, Voog E, Davis NB et al. Randomised phase II study of siltuximab (CNTO 328), an anti-IL-6 monoclonal antibody, in combination with mitoxantrone/prednisone versus mitoxantrone/prednisone alone in metastatic castration-resistant prostate cancer. Eur J Cancer 2012; 48: 85–93.
42 Mule JJ, Custer MC, Travis WD, Rosenberg SA. Cellular mechanisms of the anti-tumor activity of recombinant IL-6 in mice. J Immunol 1992; 148: 2622–2629.

43 Mullen CA, Coale MM, Levy AT, Stetler-Stevenson WG, Liotta LA, Brandt S et al. Fibrosarcoma cells transduced with the IL-6 gene exhibited reduced tumorigenicity, increased immunogenicity, and decreased metastatic potential. Cancer Res 1992; 52: 6020–6024.

44 Porgador A, Tzehoval E, Katz A, Vadai E, Revel M, Feldman M et al. Interleukin 6 gene transfection into Lewis lung carcinoma tumor cells suppresses the malignant phenotype and confers immunotherapeutic competence against parental metastatic cells. Cancer Res 1992; 52: 3679–3686.

45 Fisher DT, Chen Q, Skitzki JJ, Muhitch JB, Zhou L, Appenheimer MM et al. IL-6 trans-signaling licenses mouse and human tumor microvascular gateways for trafficking of cytotoxic T cells. J Clin Invest 2011; 121: 3846–3859.

46 Wang L, Yi T, Kortylewski M, Pardoll DM, Zeng D, Yu H. IL-17 can promote tumor growth through an IL-6-Stat3 signaling pathway. J Exp Med 2009; 206: 1457–1464.

47 Martin-Orozco N, Muranski P, Chung Y, Yang XO, Yamazaki T, Lu S et al. T helper 17 cells promote cytotoxic T cell activation in tumor immunity. Immunity 2009; 31: 787–798.

CrossMark

A targeting ligand enhances infectivity and cytotoxicity of an oncolytic adenovirus in human pancreatic cancer tissues

Yuki Yamamoto [a,c], Nobuyoshi Hiraoka [b], Naoko Goto [a], Yosei Rin [a,c], Kazuki Miura [a,c], Kenta Narumi [a], Hiroaki Uchida [c], Masatoshi Tagawa [d], Kazunori Aoki [a,*]

[a] Division of Gene and Immune Medicine, National Cancer Center Research Institute, 5-1-1 Tsukiji, Chuo-ku, Tokyo 104-0045, Japan
[b] Division of Molecular Pathology, National Cancer Center Research Institute, 5-1-1 Tsukiji, Chuo-ku, Tokyo 104-0045, Japan
[c] Laboratory of Oncology, Tokyo University of Pharmacy and Life Sciences, 432-1 Horinouchi, Hachioji, Tokyo 192-0355, Japan
[d] Division of Pathology and Cell Therapy, Chiba Cancer Center Research Institute, 666-2 Nitona-chou, Chuo-ku, Chiba 260-0801, Japan

ARTICLE INFO

ABSTRACT

The addition of a targeting strategy is necessary to enhance oncolysis and secure safety of a conditionally replicative adenovirus (CRAd). We have constructed an adenovirus library displaying random peptides on the fiber, and have successfully identified a pancreatic cancer-targeting ligand (SYENFSA). Here, the usefulness of cancer-targeted CRAd for pancreatic cancer was examined as a preclinical study. First, we constructed a survivin promoter-regulated CRAd expressing enhanced green fluorescent protein gene (EGFP), which displayed the identified targeting ligand (AdSur-SYE). The AdSur-SYE resulted in higher gene transduction efficiency and oncolytic potency than the untargeted CRAd (AdSur) in several pancreatic cancer cell lines. An intratumoral injection of AdSur-SYE significantly suppressed the growth of subcutaneous tumors, in which AdSur-SYE effectively proliferated and spread. An ectopic infection in adjacent tissues and organs of intratumorally injected AdSur-SYE was decreased compared with AdSur. Then, to examine whether the targeting ligand actually enhanced the infectivity of CRAd in human pancreatic cancer tissues, tumor cells prepared from surgical specimens were infected with viruses. The AdSur-SYE increased gene transduction efficiency 6.4-fold higher than did AdSur in single cells derived from human pancreatic cancer, whereas the infectivity of both vectors was almost the same in the pancreas and other cancers. Immunostaining showed that most EGFP+ cells were cytokeratin-positive in the sliced tissues, indicating that pancreatic cancer cells but not stromal cells were injected with AdSur-SYE. AdSur-SYE resulted in a stronger oncolysis in the primary pancreatic cancer cells co-cultured with mouse embryonic fibroblasts than AdSur did. CRAd in combination with a tumor-targeting ligand is promising as a next-generation of oncolytic virotherapy for pancreatic cancer.

© 2014 Elsevier B.V. All rights reserved.

1. Introduction

Pancreatic cancer is the leading cause of cancer death, and it is considered one of the most lethal cancers in Japan as well as in the Western countries [1–3]. Despite the recent advances in therapeutic and diagnostic modalities [4,5], overcoming it remains one of the most formidable challenges in oncology today. Complete surgical resection has traditionally been considered the only curative treatment, but high rates of local and systemic failure persist in patients who undergo curative resections, and a 5-year survival rate is less than 5% [1]. This high mortality is due to the high incidence of metastatic disease at the time of diagnosis, a fulminant clinical course and the lack of adequate systemic therapies. In the locally advanced cases also, the development of strategies to strongly control local lesions and prevent distant metastases is an important issue. In spite of the fact that many studies have been tried to improve the outcomes, a novel approach is needed [3,5].

The conditionally replicative adenoviruses (CRAds), which are genetically programmed to replicate within tumor cells but not in normal cells and directly induce cytotoxic effects via cell lysis, are currently being explored in preclinical and clinical studies of various cancers such as head and neck cancer, pancreatic cancer, ovarian cancer, prostate cancer and malignant glioma [6–8]. Progress in the clinical studies of CRAds for solid cancers has been clarifying the need for two issues to be addressed [6,7,9]. First, tumor oncolytic activity should be enhanced to achieve any significant antitumor response. Since, in general, the oncolytic activity of CRAds is closely related with the infectious ability to the targets, the improvement of viral infectivity to tumors is necessary. However, an undesirable viral spread to adjacent tissues should be strictly limited around the virus-replicating tumors to reduce any adverse effect. In addition, CRAds leak from the tumors into systemic

circulation often causes ectopic infection to vital organs such as the liver [10]. Therefore, suppression of naïve tropism for the reduction of unnecessary infection in non-target tissues and organs, and the reinforcement of a tumor-targeting potential in combination with the reduced tropism should solve the issues of conventional CRAds therapy [10,11].

Most of the presently used CRAds are based on serotype 5 (Ad5), whose entry into susceptible cells requires two distinct and sequential steps. The initial step is facilitated by an interaction of the fiber protein with its cellular receptor coxsackievirus and adenovirus receptor (CAR) [12]. Following attachment to CAR, internalization of the virus is promoted by the interaction of the penton base with αv integrins on the cell surface [12]. Retargeting has been achieved by direct genetic modifications of the capsid proteins: targeting ligands can be incorporated into the C-terminal and HI-loop of fiber proteins ablated for native tropism through the loss of binding with CAR and/or αv integrins [6,12]. However, the redirection of adenovirus vectors by engineering the capsid-coding region has shown limited success because proper targeting ligands are generally unknown. To overcome this limitation, we have developed a system for producing adenoviral libraries displaying a variety of peptides on the HI-loop of the fiber knob, and its screening has led to successful selections of several particular adenoviral vectors with high infectivity in target cells [13–17]. SYENFSA (SYE) is one of the selected sequences from the library by screening on the AsPC-1 pancreatic cancer cell line *in vitro*, and the adenovirus displaying the sequence showed higher infectivity in four of five pancreatic cancer cell lines [15].

To date, 2 types of CRAds have been developed. Type I is for introducing a mutation in the E1 region, and the function of these missing genes may be complemented by genetic mutation in tumor cells such as p53 mutation. Type II is for constructing viruses in which the transcription of E1 genes is restricted to tumor cells by either a tumor or tissue-specific promoter [6–8]. Survivin (Sur) is an anti-apoptotic protein involved in mitotic regulation during embryotic and fetal development, but its expression is generally undetectable in terminally differentiated adult tissue [18]. The promoter activity, largely silent in normal cells, is prominently expressed in tumor tissues including pancreatic cancer, and cells transfected with a reporter gene under the control of a Sur promoter exhibit cancer-specific activity *in vitro* and *in vivo* [19,20]. Therefore, CRAds, in which the transcription of E1 genes is restricted to tumor cells by the Sur promoter, were widely studied [21]. In this study, we constructed a Sur promoter-regulated CRAd displaying the pancreatic cancer-targeting sequence SYE (AdSur-SYE) to enhance oncolysis and secure safety. The therapeutic usefulness of AdSur-SYE was validated in surgical specimens of human pancreatic cancer as a preclinical study.

2. Materials and methods

2.1. Cell lines

Used in this study were a human embryonic kidney cell line (293), human pancreatic cancer cell lines (AsPC-1, BxPC-3, Panc-1 and MIAPaCa-2), a human prostate cancer cell line (PC3), a human dermal fibroblast and a mouse embryonic fibroblast (MEF). All the cancer cell lines were obtained from the American Tissue Culture Collection (ATCC; Rockville, MD, USA). Fibroblast was purchased from PromoCell GmbH (Heidelberg, Germany) and MEF was from ReproCell (Kanagawa, Japan). 293 cells, MIAPaCa-2 cells and MEFs were cultured in Dulbecco's modified eagle's medium (DMEM; Wako Pure Chemical Industries, Ltd., Osaka, Japan) with 10% fetal bovine serum (FBS); pancreatic cancer cell lines except for MIAPaCa-2 and PC3 were cultured in an RPMI-1640 medium (Nissui Pharmaceutical, Tokyo, Japan) with 10% FBS. Fibroblasts were cultured in the fibroblast growth medium (PromoCell GmbH). The 293–38 is a high-efficiency virus-producing clone of 293 cells [13].

2.2. Human surgical specimens

Surgical specimens (15 pancreatic ductal adenocarcinomas, 1 intraductal papillary mucinous neoplasm, 1 metastasis of renal cancer, 1 gallbladder cancer, 1 duodenal cancer, 6 pancreases and 1 liver) were obtained according to the Declaration of Helsinki Principles and the guideline of the Ethics Committee of the National Cancer Center (Tokyo, Japan). None of the patients had received any prior therapy. Tissues were processed into single cells or small pieces (1–4 mm in diameter), and were cultured in RPMI-1640 medium with 10% FBS.

2.3. Plasmids and recombinant adenovirus vectors

The 0.5-Kb survivin regulatory region [20] was inserted into the pGL3 basic vector (Promega, Madison, WI, USA) that contains the firefly luciferase gene, and designated as a pSur-Luc. A pRL-SV40 plasmid (Promega) expresses *Renilla* luciferase gene under the control of a SV40 promoter.

Adenovirus vectors were constructed as previously described [14,15,22]. The adenovirus vectors except for Ad-EGFP and AdΔE1-AP include 4 point mutations in the AB-loop of the fiber knob that reduces CAR binding. Ad-EGFP and AdΔE1-AP have a wild type of fiber. The AdSur-SYE and AdSur contain a 0.5-Kb survivin regulatory region upstream of the adenoviral E1 gene [20]. The AdΔCAR-SYE, AdΔCAR and Ad-EGFP contain a wild type of E1 region. The AdΔCAR-SYE, AdSur-SYE and AdLucEGFP-SYE have a SYE sequence in the HI-loop on the fiber knob [15,16]. The virus vectors contain a CMV promoter, the enhanced green fluorescent protein (EGFP) gene and a SV40 poly(A) signal in place of the E3 region, except for the AdΔE1-AP, AdLucEGFP and AdLucEGFP-SYE. In these viruses, the E1 gene is replaced with the CMV promoter-driven alkaline phosphatase or luciferase-EGFP fusion gene (LucEGFP), respectively (Fig. 1). The adenovirus vectors were expanded in the 293–38 cells. Physical particle concentration (viral particles (vp)/ml) of virus preparation was determined by optical absorbance (OD_{260}) [23].

2.4. Assay for luciferase activity

The cells were seeded at 1×10^5 per well in 24-well plates and transfected with both of pSur-Luc and pRL-SV40 by the lipofection method (Lipofectamine 2000 Reagent; Life Technologies Corp., Carlsbad, CA, USA). The cells were harvested with 100 μl of reporter lysis buffer (Promega) 48 h after the transfection. The light units of firefly and *Renilla* luciferase activities were assessed by dual luciferase reporter assay (Promega) using a luminometer (MiniLumat LB9506; EG&G Gerthold, Vilvoorde, Belgium). The sliced tissues prepared from surgical specimens of human pancreatic cancer (~1 mm in diameter) were infected with 3×10^9 vp of AdLucEGFP-SYE and AdLucEGFP. Twenty-four hours after the infection, the tissues were lysed with an equal volume of reporter lysis buffer. Twenty microliters of cell lysates were mixed with 100 μl of luciferase assay substrate (PicaGene; Toyo Ink CO., LTD., Tokyo, Japan). The light units of luciferase activity were measured using a luminometer (MiniLumat LB9506).

2.5. In vitro cell growth assay

The cells were seeded at 3×10^3 per well in 96-well plates and infected with viruses at 300, 1×10^3, 3×10^3, 1×10^4 and 3×10^4 vp/cell. The 1×10^4 of single cells prepared from surgical specimens of pancreatic cancers were co-cultured with 1×10^4 of MEF as feeder cells per well in 96-well plates and were infected with viruses at 1×10^3, 3×10^3, 1×10^4 and 3×10^4 vp/cell. The cell numbers were assessed by a colorimetric cell viability assay using a water-soluble tetrazolium salt (Tetracolor One; Seikagaku Corp., Tokyo, Japan). The absorbance was determined by spectrophotometry using a wavelength of 450 nm with 600 nm as a reference.

2.6. In vivo tumor growth

Five-week-old female BALB/c nude mice were purchased from Charles River Japan, Inc. (Kanagawa, Japan), and were housed under sterilized conditions. Animal studies were carried out according to the Guideline for Animal Experiments of the National Cancer Center Research Institute and approved by the Institutional Committee for Ethics in Animal Experimentation. BxPC-3 and PC3 cells (5×10^6) were injected subcutaneously into the nude mice. When tumor mass was established (~0.6 cm in diameter), 50 µl of a viral solution (0.5 or 2×10^{10} vp) was directly injected into the tumor. The short (r) and long (l) diameters of the tumors were measured and the tumor volume of each was calculated as $r^2 \times l \times 1/2$.

2.7. Detection of adenovirus DNA from cells

DNA was extracted from the cells 3 and 5 days after the virus infection using NucleoSpin Tissue (Macherey-Nagel, GmbH & Co.,
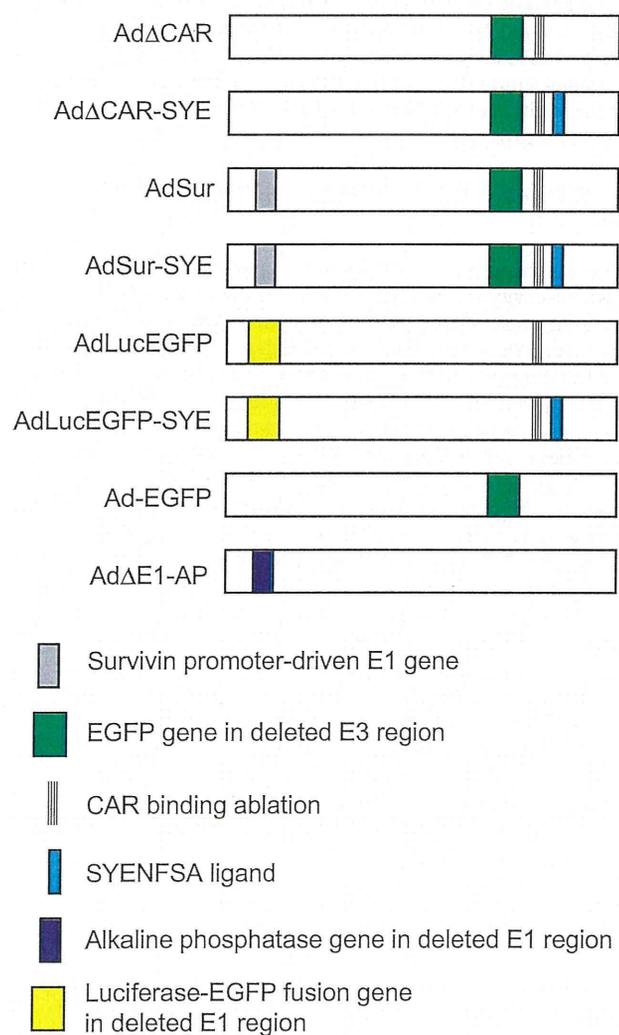

Fig. 1. Design of adenovirus constructs displaying a pancreatic-cancer targeting ligand. In adenovirus vectors except for Ad-EGFP and AdΔE1-AP, 4 point mutations were inserted in the AB-loop to reduce the CAR binding. In AdSur and AdSur-SYE, E1 gene is regulated by survivin promoter. In AdΔE1-AP, AdLucEGFP and AdLucEGFP-SYE, the E1 gene is replaced with CMV promoter-driven alkaline phosphatase or luciferase-EGFP fusion gene, respectively. The Ad-SYE, AdSur-SYE and AdLucEGFP-SYE display a pancreatic cancer targeting sequence SYENFSA on the fiber knob.

Duren, Germany). Adenoviral DNA was measured by SYBR Green real-time PCR using Eco™ Real-Time PCR system (Illumina Inc., San Diego, CA, USA). Briefly, 50 ng of extracted DNA was added to a final volume of 10 µl/reaction containing 1 × SYBR Green PCR Master Mix (Applied Biosystems Japan, Tokyo, Japan) and 100 nM of the primers; E4 upstream (5′-GGAGTGCGCCGAGACAAC-3′) and the downstream (5′-ACTACGTCCGGCGTTCCAT-3′), which detect a 68-bp region in E4 [16]. Thermal cycling conditions were as follows: initial denaturation at 95 °C for 10 min, and then 40 cycles at 95 °C for 10 s and at 60 °C for 30 s.

2.8. Detection of adenovirus genome from tumors and organs

DNA was extracted from the tumors and organs such as the liver, spleen, pancreas and lung 2 days after the intratumoral injection of an adenovirus solution (2×10^{10} vp) using Sepagene (Sanko Junyaku Co. Ltd., Tokyo, Japan). To quantitatively analyze the viral genome, SYBR Green real-time PCR was performed with the same E4 primers. A final volume of 10 µl/reaction containing 1 × SYBR Green Master Mix (Applied Biosystems Japan), 100 nM primers and 50 ng of extracted DNA was applied to the real-time PCR. For the standard curve to quantify the E4 copy numbers, E4 template DNA with a known copy number (2.4×10–2.4×10^6) was also analyzed. Thermal cycling conditions were as follows: initial denaturation at 95 °C for 10 min, and then 40 cycles at 95 °C for 10 s and at 60 °C for 30 s.

2.9. Flow-cytometry

Flow-cytometry was performed to assess the percentage of EGFP+ cells. The cells were harvested 24 h after the viral infection, and were stained with LIVE/DEAD cell vitality assay kit (Life Technologies Corp.) for the selection of live cells followed by fixation with 4% paraformaldehyde (Wako Pure Chemical Industries, Ltd.) for 20 min at room temperature. For an epithelial cell marker MUC-1 staining, after the fixation, the cells were stained with monoclonal mouse α-human MUC-1 antibody (E29; Dako, Glostrup, Denmark) for 30 min at room temperature followed by staining with Alexa Fluor 647-goat anti mouse IgG (Life Technologies Corp.), and analyzed by FACS Calibur (BD Biosciences, San Jose, CA, USA).

2.10. Immunohistochemistry

The surgical specimens of human pancreatic cancer were processed into sliced pieces (~4 mm in diameter), and were infected with adenoviruses. Twenty-four hours later, the tissues were fixed in 4% paraformaldehyde at room temperature overnight. The cryostat tissue sections (4 µm) were mounted on glass slides and were subjected to immunohistochemistry to detect a cytokeratin. The sections were stained with monoclonal mouse α-human pancytokeratin antibody (AE1/AE3; Dako) and then with biotinylated anti-mouse IgG (Vector Laboratories, Burlingame, CA, USA) and streptavidin-conjugated Alexa Fluor 555 (Life Technologies Corp.). All the sections were counter-stained with DAPI (4′, 6-diamidino-2-phenylindole, dihydrochloride; Life Technologies Corp.).

2.11. Statistical analysis

Comparative analyses of the data were performed by the Student's t-test, using SPSS statistical software (SPSS Japan Inc., Tokyo, Japan). The differences were considered statistically significant when the P value was <0.05.

3. Results

3.1. High infectivity of AdΔCAR-SYE in human pancreatic cancer tissues

We previously reported that the replication-competent adenovirus with a wild type E1 region, which displayed a SYENFSA ligand (AdΔCAR-SYE), showed higher gene transduction efficiency in several other pancreatic cancer cell lines compared with the untargeted adenovirus (AdΔCAR) [15,16]. In this study, to examine whether the ligand-mediated high infectivity is recognized in the human pancreatic cancer tissues as well, the surgical specimens were first infected with AdΔCAR-SYE or AdΔCAR. Flow-cytometry showed that AdΔCAR-SYE increased the frequency of EGFP+ cells 3.8-fold higher than AdΔCAR did in pancreatic cancer but not in the other types of cancer (Supplementary Fig. 1).

Next, the sliced tissues (~1 mm in diameter) were infected with luciferase-expressing adenoviruses. AdLucEGFP-SYE showed a higher luciferase activity than did the untargeted virus (AdLucEGFP) (Supplementary Fig. 2). The results confirmed the specific and high infectivity of an adenovirus vector displaying the SYE ligand not only in pancreatic cancer cell lines but also in human pancreatic cancer tissues.

3.2. Construction of a cancer-targeted adenovirus regulated by survivin promoter

Next, we constructed a CRAd displaying the targeting ligand SYE on the fiber knob. To address the relevance of a survivin promoter as the candidate tumor targeting promoter, the cancer cell lines and a primary culture of human dermal fibroblasts were transfected with pSur-Luc and pRL-SV40. The relative activity of survivin promoter to SV40 promoter was significantly higher in the pancreatic cancer cell lines than in PC3 cells and fibroblasts (Fig. 2A). Then, to examine the infectivity of CRAd displaying the SYE ligand, the cancer cell lines were infected with AdSur-SYE or AdSur. Flow-cytometry showed a higher infectivity in all 4 pancreatic cancer cell lines infected with AdSur-SYE than those infected with AdSur in a dose-dependent manner, whereas in the PC3 cells and fibroblasts, the frequencies of EGFP+ cells in the AdSur-SYE-infected cells were comparable or less than that in the AdSur-infected cells (Fig. 2B and C). To confirm the virus replication in the cells infected with CRAds, we analyzed the copy number of the virus genome per cell by the real-time PCR method 3 and 5 days after the infection at 1×10^3 vp/cell. The adenovirus DNA rapidly increased in the AdSur-SYE-infected BxPC-3 cells, whereas it was not changed in the PC3 cells and fibroblasts (Fig. 2D).

3.3. Antitumor effect of a cancer-targeted conditionally replicative adenovirus

To examine whether the addition of targeting potential to CRAd results in an effective cell killing, cancer cell lines were infected with viruses. An *in vitro* cell growth assay showed that the AdSur-SYE markedly suppressed the growth of all 4 pancreatic cancer cell lines compared with AdSur, while the cytotoxic activity of AdSur-SYE was higher than that of Ad-EGFP. In PC3 cells and fibroblasts, the difference of cell growth inhibition between AdSur and AdSur-SYE was small (Fig. 3A).

Then, to investigate the *in vivo* efficacy of targeted CRAd, viruses were directly injected into BxPC-3 and PC3 subcutaneous tumors. The injection of AdSur-SYE effectively suppressed the BxPC-3 tumor growth more than AdSur did, and the higher dose of AdSur-SYE suppressed the tumor growth more efficiently than the Ad-EGFP, whereas the *in vivo* antitumor effect of AdSur was larger than that of AdSur-SYE in the PC3 tumors (Fig. 3B). The AdSur-SYE resulted in the central necrosis in the BxPC-3 tumors (Fig. 3C). To examine whether the viruses replicate and spread in the tumor tissues, the transgene expression was compared in AdΔE1-AP, AdSur and AdSur-SYE-injected tumors at day 2 and day 6 after injection. The expression in AdΔE1-AP- and AdSur-injected BxPC-3 tumors decreased at day 6 compared to day 2, whereas a marked EGFP expression was observed in AdSur-SYE-injected tumors at day 6 (Fig. 3D), indicating that AdSur-SYE more effectively proliferate and spread in the tumors. EGFP+ cells were not detected in the adjacent skin and skeletal muscle (data not shown). In addition, the viral genome copy number in BxPC-3 tumors at days 2 and 6 was examined by the real-time PCR method, showing that the copy number of AdSur-SYE in the tumors significantly increased as compared with those of AdΔE1-AP and AdSur (Fig. 3E). All treated mice looked healthy during the course of the experiments, and blood chemistry showed no abnormal values in the treated mice at 4 weeks.

3.4. Ectopic infection of organs after intratumoral injection of adenoviruses

The replication of the adenovirus in the tumors results in an ectopic infection of organs through leakage into systemic circulation [10,15]. To evaluate the distribution of adenovirus genome in organs, various organs and subcutaneous tumors were subjected to real-time PCR 2 days after the intratumoral injection of viruses. The adenoviral genome copy number of AdSur-SYE in tumors was significantly elevated as compared with that of AdSur and was similar with Ad-EGFP, whereas the copy numbers of AdSur-SYE in organs were significantly less than those of AdSur and Ad-EGFP, indicating that the addition of SYE ligand decreased the ectopic undesirable infection of organs (Fig. 4).

3.5. Infectivity of AdSur-SYE in surgical specimens of human pancreatic cancer

To examine whether an addition of a targeting ligand in CRAd leads to high infectivity and oncolytic activity in the human pancreatic cancer tissues, the single cells prepared from surgical specimens were infected with AdSur-SYE or AdSur, and the percentage of EGFP+ cells was analyzed by flow-cytometry 24 h after the infection. More than 60% of the single cells were MUC-1 positive, suggesting that a major population of live cells was pancreatic ductal adenocarcinoma cells (Fig. 5A). The infectivities of AdSur-SYE were 6.4-fold at 1×10^3 vp/cell and 6.2-fold at 1×10^4 vp/cell higher compared with those of AdSur in the pancreatic cancers, whereas the infectivities of AdSur-SYE and AdSur were almost the same in the other cancers, the pancreas and liver (Fig. 5B).

Next, the sliced tissues of pancreatic cancers were infected with AdSur-SYE or AdSur. EGFP+ cells were detected on the surface of the AdSur-SYE-infected tissues, whereas the EGFP+ cells were not detected in the AdSur-infected tissues. EGFP+ cells in AdSur-SYE-infected tissue seemed to be pancreatic cancer cells in H&E staining of the same section (Fig. 5C). Since pancreatic cancer cells on the tissue slides were not clearly stained by the immunohistochemistry of MUC-1, cytokeratin was immunostained. The staining showed that most EGFP+ cells in the AdSur-SYE-infected tissues were positive for cytokeratin, indicating that the cells infected with the virus were pancreatic cancer cells but not stromal cells such as endothelial cells and immune cells (Fig. 5D).

3.6. Oncolytic activity of AdSur-SYE in surgical specimens of human pancreatic cancer

Finally, to examine the oncolytic effect of AdSur-SYE, the single cells prepared from 4 patients with pancreatic cancer were co-cultured with MEFs, and were infected with viruses. Immunocytochemistry showed that several MUC-1+ cells aggregated and grew as islands on the MEFs at day 6 (Fig. 6A), indicating that a significant population of cells prepared from surgical specimens was alive for at least 6 days. The number of EGFP+ cells in AdSur-SYE-infected pancreatic cancer cells was significantly larger as compared with the AdSur-infected cells (Fig. 6B), and many EGFP+MUC-1+ cells were detected by ArrayScan VTI HCS Reader (Thermo Scientific, MA, USA) (Fig. 6C). An *in vitro* cell growth assay
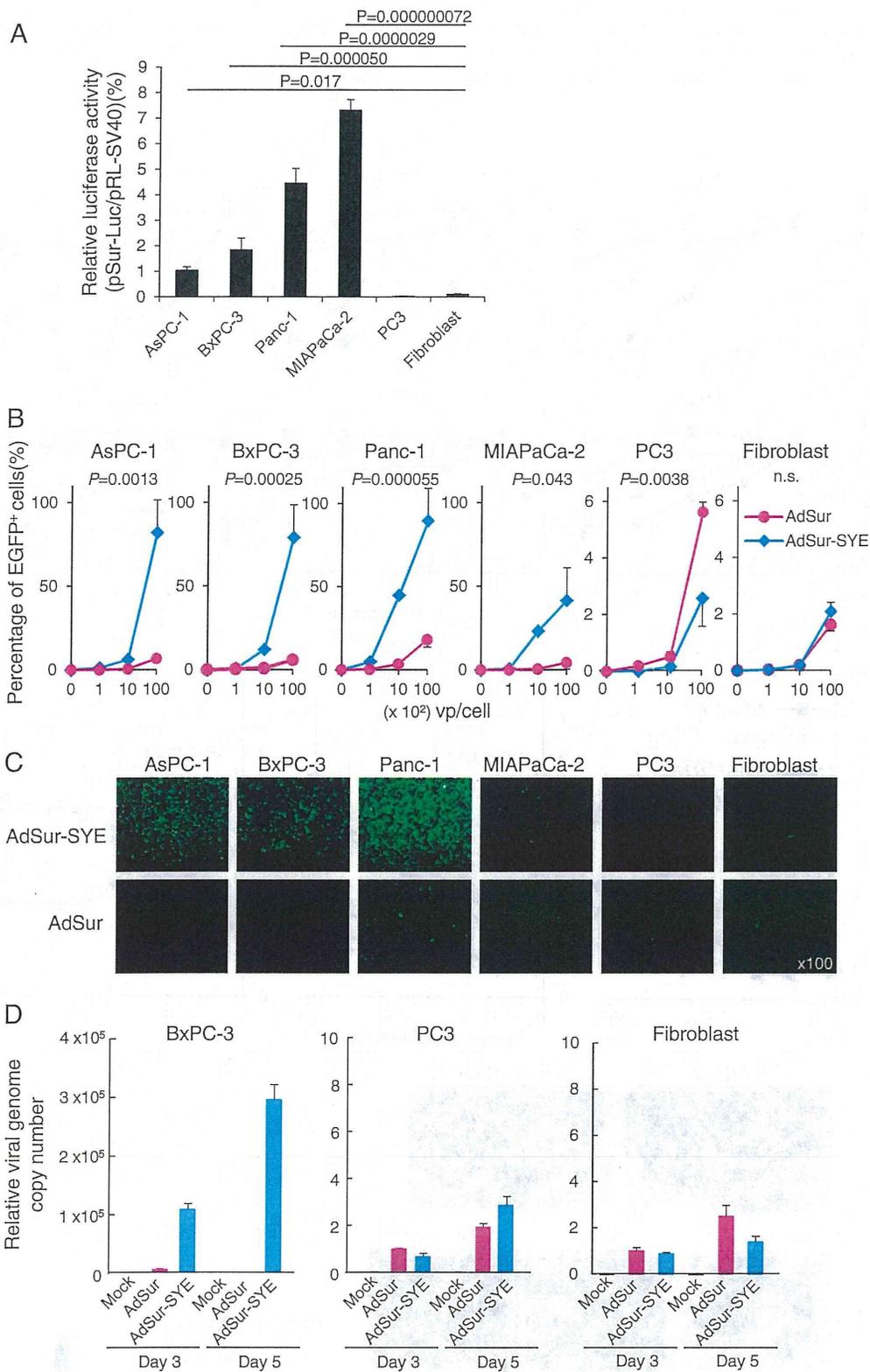
Fig. 2. Activity of survivin promoter and infectivity of AdSur-SYE in pancreatic cancer cell lines. A) The activity of survivin promoter in human pancreatic cancer cell lines. The cells were transfected with pSur-Luc and pRL-SV40, and 48 h later the luciferase activity was measured. The relative luciferase activity (the light unit of cells transfected with pSur-Luc/that with pRL-SV40) is presented. The assays (carried out in 5 wells) were repeated three times and the mean ± standard deviation was plotted. B) Infectivity of AdSur-SYE in pancreatic cancer cell lines. The cells were infected with AdSur-SYE or AdSur, and 24 h later the EGFP⁺ cells were analyzed by flow-cytometry (n = 4). C) Photographs of cell lines infected with viruses at 1×10^4 vp/cell. D) The replication of adenoviral DNA in the cells. BxPC-3, PC3 cells and fibroblasts were infected with AdSur-SYE or AdSur at 1×10^3 vp/cell, and 3 and 5 days later the adenoviral DNA was analyzed by real-time PCR analysis (n = 3). The viral genome copy number was normalized to β-actin gene. The copy numbers at indicated viruses and days are shown as compared with that of AdSur at day 3.

showed that the proliferation was suppressed in cells infected with viruses in a dose-dependent manner, while the AdSur-SYE most effectively suppressed the growth of all 4 pancreatic cancer cells as compared with the AdSur, and that the cytotoxicity of AdSur-SYE was equal to or greater than that of Ad-EGFP (Fig. 6D). The results demonstrated that the pancreatic cancer-targeted CRAd showed a higher infectivity and oncolytic activity than untargeted CRAd in human pancreatic cancer tissues as well.
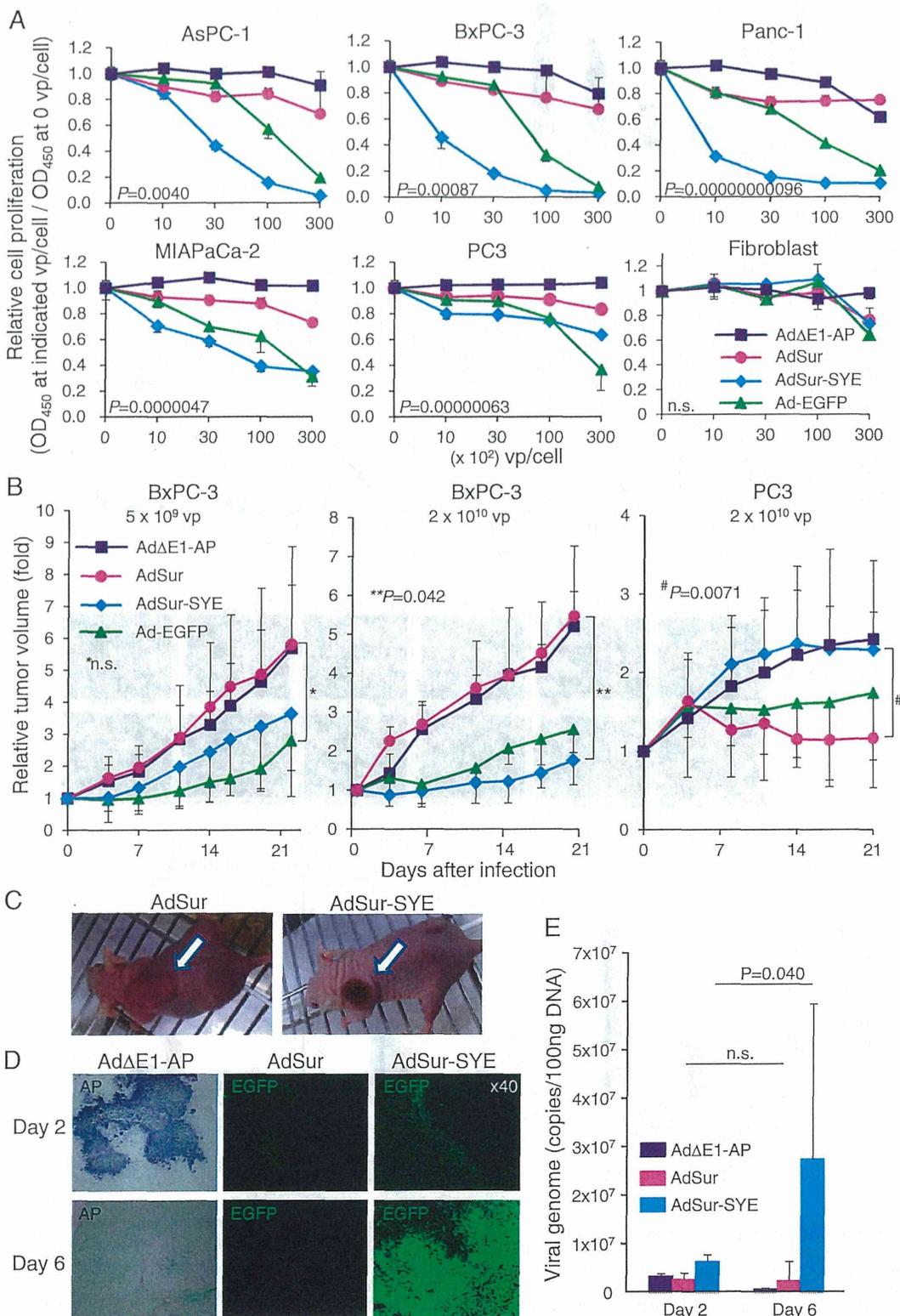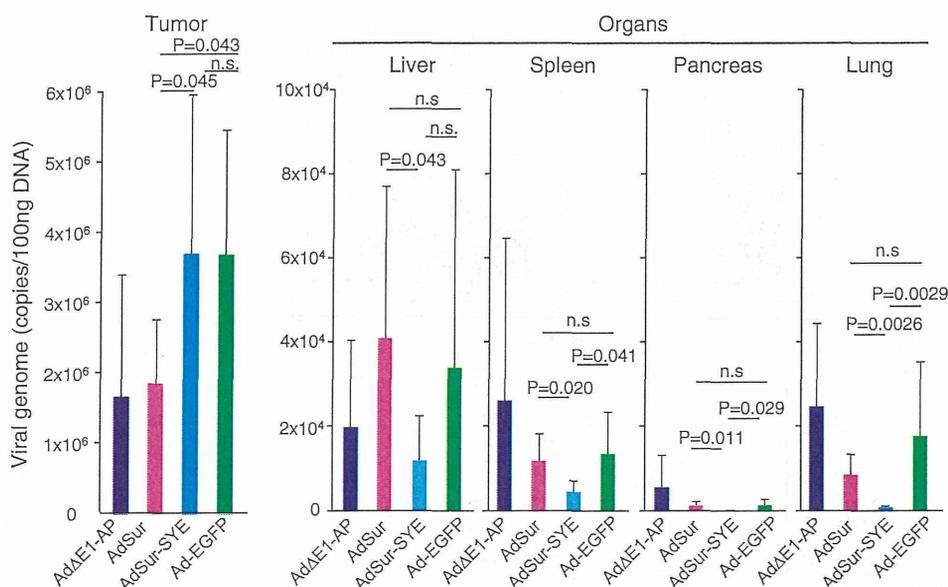
Fig. 4. Distribution of adenoviruses after intratumoral injection. DNA from the tumors and organs of AdΔE1-AP-, AdSur-, AdSur-SYE- or Ad-EGFP-injected mice was subjected to real-time PCR, and adenoviral genome copy numbers were analyzed (tumor; n = 6, liver; n = 6, spleen; n = 6, pancreas; n = 3, lung; n = 3).

4. Discussion

We previously reported that a replication-competent adenovirus displaying the SYE ligand exerted a potent cell killing in several pancreatic cancer cell lines [15]. However, the previous vectors contained a wild E1 region, which was not a typical CRAd, and it was not applicable in the clinical setting. In this study, we combined the pancreatic cancer-targeting ligand with CRAd, which is regulated by the survivin promoter, and demonstrated that CRAds equipped with a cancer-targetability showed a high infectivity and oncolytic activity in pancreatic cancer cell lines, mouse xenograft tumor models and human surgical specimens of pancreatic cancer.

The SYE sequence was selected by screening on the AsPC-1 pancreatic cancer cell line, and the infection of targeted vectors was considered to be mediated by specific receptors on target cells [15]. Since the expression levels and kinds of cell surface receptors may be substantially different between in vitro cell culture cells and in vivo tumor tissue, the infectivity in the human pancreatic cancer specimens may be different from those in the cell lines. The fact that the SYE ligand selected by in vitro cell line screening showed a high infectivity in human pancreatic cancer tissues also indicates that our screening strategy using cell lines is useful for identifying the ligand sequences, which are applicable in the clinical setting.

Since the SYE-mediated enhancement of gene transduction was observed in several pancreatic cancer cell lines (Fig. 2B and C), the cognate receptor for SYE sequence may be shared by these pancreatic cancer cell lines. Identification of the receptors is useful for understanding the molecular characteristics of the target cells and can be applied for diagnosis, such as the detection of a relapse of the disease. At present, we are developing a receptor identification system using microarray technology.

Although AdSur-SYE showed significantly stronger antitumor effects for pancreatic cancer cells, there were some discrepancies between in vitro culture and subcutaneous tumors. AdSur-SYE mediated more efficient tumor cell killing than Ad-EGFP in AsPC-3, BxPC-3 and Panc-1 cells, whereas tumor growth rates of subcutaneous BxPC-3 tumors were similar between AdSur-SYE and Ad-EGFP groups (Fig. 3A and B). The expression level of an unknown cognate receptor for SYE ligand in pancreatic cancer cell lines might be higher than that in BxPC-3 subcutaneous tumors. In addition, the AdSur-SYE showed a pancreatic cancer cell-specific infectivity, whereas the Ad-EGFP has a broad spectrum of infectivity due to the wild type of fiber. The pancreatic cancer cells as well as stromal cells such as fibroblasts and vascular endothelial cells may be infected with Ad-EGFP, which leads to the strong antitumor effect. Besides, AdSur effectively suppressed the growth of PC3 subcutaneous tumors than AdSur-SYE did (Fig. 3B). This antitumor effect of AdSur was confirmed in 2 independent experiments, and in our previous report also, a replication-competent adenovirus displaying no peptide (AdΔCAR) showed the stronger antitumor effect for PC3 tumors than the SYE-displaying adenovirus (AdΔCAR-SYE) [15]. Although the precise reason is unknown, PC3 tumors may be infected with AdSur via another unknown specific receptor, and the insertion of the SYENFSA sequence might disturb the AdSur infection due to the conformational change of a particular portion in fiber knob.

The key prerequisite for an efficient oncolytic virus is the restriction of virus replication in tumor cells. Although the replication and spreading of CRAds are restricted to tumor tissue in theory, several levels of additional safety devices are definitely required: the engineering of an adenovirus capsid to restrict infection for tumor cells being the first safety device, and E1 manipulation to limit replication in the tumors being the second one. In our vectors, CAR binding was ablated to reduce the naïve tropism, and, in fact, the intratumoral injection of AdSur-SYE

Fig. 3. Cytotoxic activity of AdSur-SYE in pancreatic cancer cells. A) Suppression of cell growth in pancreatic cancer cell lines. The cells were infected with viruses, and 5 days later a cell growth assay was performed. The relative cell growth (OD_{450} of cells at indicated vp/cell/that at 0 vp/cell) is shown. The assays (carried out in 4 wells) were repeated two times and the mean ± standard deviation was plotted. P value: AdSur-infected cells versus AdSur-SYE-infected cells at 3×10^4 vp/cell. B) Growth suppression of BxPC-3 subcutaneous tumors. Adenovirus vectors were injected into BxPC-3 and PC3 subcutaneous tumors inoculated in immune-incompetent mice. (Left) 5×10^9 vp of adenoviruses was injected into the BxPC-3 tumors (n = 8). (Middle) 2×10^{10} vp of adenoviruses was injected into the BxPC-3 tumors (n = 8). (Right) 2×10^{10} vp of adenoviruses was injected into the PC3 tumors (n = 7). C) Photographs of representative tumors 21 days after virus injection. BxPC-3 tumors were injected with 2×10^{10} vp of adenoviruses. D) Transgene expression in BxPC-3 subcutaneous tumors. Frozen sections of tumors were examined at days 2 and 6 after the injection of viruses (2×10^{10} vp) under fluorescence microscopy. The AdΔE1-AP-injected tumors were stained for AP activity (BCIP/NBT kit; Zymed Laboratories Inc., CA), and the sections were counterstained with methyl green. AP; alkaline phosphatase staining. E) The replication of adenovirus in tumors. Adenoviral genome copy numbers in tumors at days 2 and 6 after the injection were examined by the real-time PCR method.
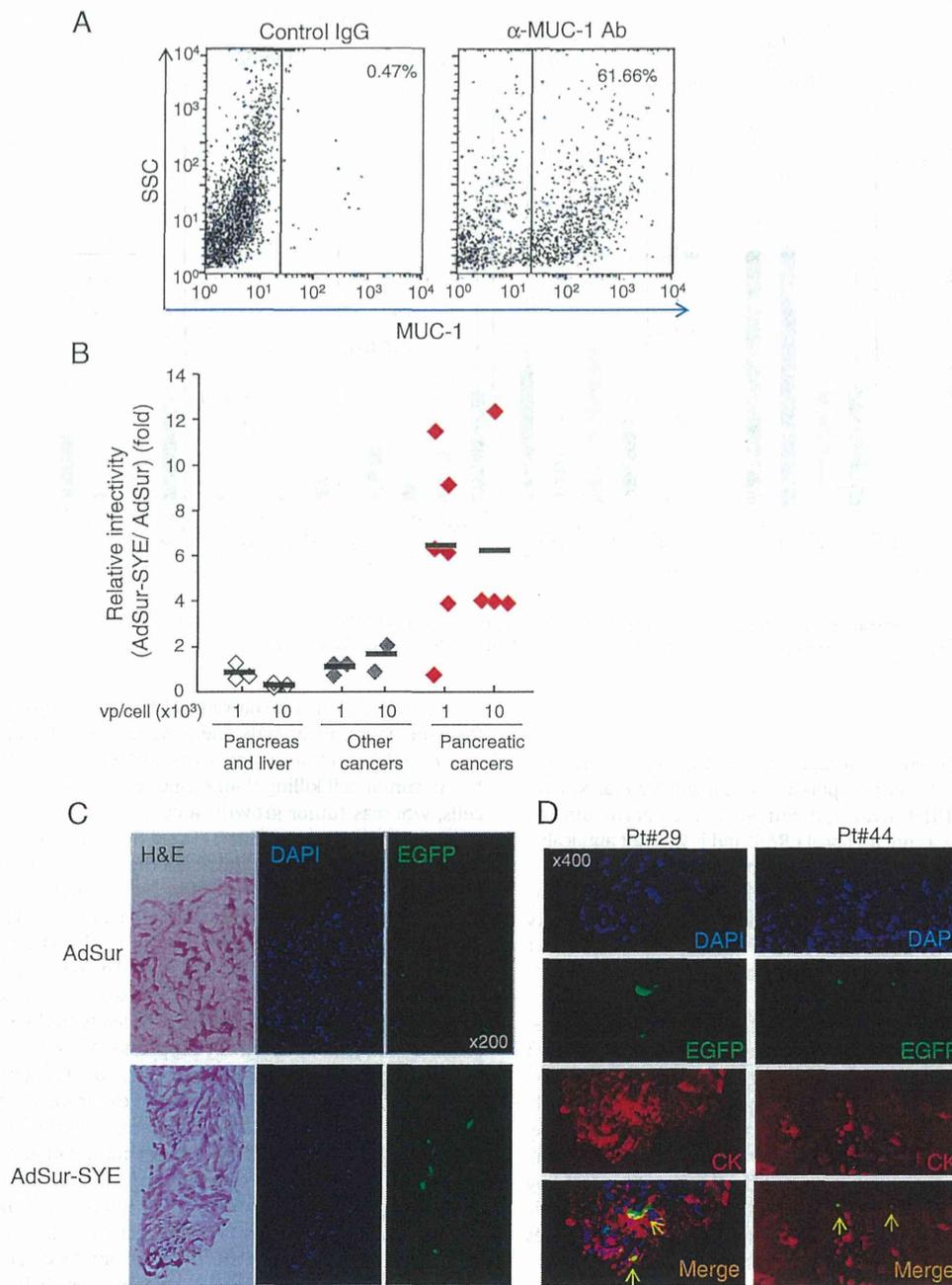
Fig. 5. Infectivity of AdSur-SYE in human pancreatic cancer tissues. Tumor cells were prepared from the surgical specimens of human pancreatic cancer. A) MUC-1^{+} cells in the surgical specimens. Tumor cells were stained with α-MUC-1 antibody followed by Alexa Fluor 647. Ab: antibody. B) The detection of EGFP^{+} cells by flow-cytometry. Tumor cells were infected with AdSur or AdSur-SYE at 1×10^3 and 1×10^4 vp/cell, and 24 h later EGFP^{+} cells were analyzed by flow-cytometry. The relative frequency of EGFP^{+} cells (the percentage of EGFP^{+} cells infected with AdSur-SYE/that with AdSur) is presented. Pancreas; n = 2. Liver; n = 1. Other cancer; n = 2 (gallbladder cancer and duodenal cancer). Pancreatic cancer; n = 6 (pancreatic ductal adenocarcinoma). C) EGFP expression of sliced tissues infected with adenoviruses. The sliced tissues (Patient number: Pt# 29) were infected with 1×10^{10} vp of AdSur or AdSur-SYE, and 24 h later the tissues were fixed by 4% paraformaldehyde, and frozen sections were observed under fluorescent microscopy. D) Cytokeratin staining of sliced tissues infected with AdSur-SYE. The sliced tissues (Pt#29 and Pt#44) were infected with 1×10^{10} vp of AdSur-SYE, and after fixation, frozen sections were stained with α-pancytokeratin antibody. CK; cytokeratin Arrows; EGFP[+] cytokeratin^{+} cells.

did not increase the infection of the adjacent tissues. In general, the additional ablation of binding sites with integrin and heparan sulfate proteoglycans from the adenoviral capsid may be useful to further reduce naïve tropism [24]. Although in this study an ectopic infection in distant organs of intratumorally injected AdSur-SYE was decreased compared with AdSur (Fig. 4), this decrease may be due to the reduced amount of viruses leaking from the tumor because of the enhanced transduction efficiency of AdSur-SYE in tumors. If the same amount of virus was intravenously injected, a level of ectopic infection in distant organs should be comparable between AdSur-SYE and AdSur as previously reported [15]. It was recently reported that coagulation factor (F) X binds the hypervariable regions (HVR) of the hexon in an adenovirus, leading to liver infection [25,26]. The factor X enhances liver transduction by adenovirus vectors due to the protection of adenovirus from attack by the classical complementary pathway [27]. Therefore, a targeted adenovirus constructed on a mutant hypervariable region backbone to